COMMUNICATION

Overcharge performance of 3,7-disubstituted N-ethylphenothiazine derivatives in lithium-ion batteries†

Selin Ergun, Corrine F. Elliott, Aman Preet Kaur, Sean R. Parkin and Susan A. Odom*

3,7-Disubstituted N-ethylphenothiazine derivatives were synthesized as redox shuttle candidates for lithium-ion batteries. Battery cycling results show that three derivatives prevent overcharge.

Lithium-ion batteries (LIBs) are the most common energy storage systems for portable electronic devices due to their high energy densities, low rates of self-discharge, long cycle lifetimes, lack of memory effect, and high rate capabilities.[1,2] However, safety issues associated with LIBs are major obstacles for large scale applications. During overcharge, a condition in which cell potential rises above the end-of-charge state of the cathode, overdelithiation can lead to decreased capacities, and increased temperatures can lead to fires and explosions.[3,4] Several techniques have been proposed and applied to prevent overcharge, including the use of electrolyte additives called redox shuttles, which prevent cell voltage from rising beyond the additive's oxidation potential through redox reactions at the electrode/electrolyte surfaces, shuttling current through the electrodes instead of further charging the battery.[5–8]

For redox shuttles to be utilized in overcharge protection, their oxidation potentials should be slightly higher than the end-of-charge potential of the cathode; this prevents their interference with battery charging and enables their activation soon after overcharge occurs. Hundreds of compounds have been tested as redox shuttles;[2,9–13] however, most tested candidates are not commercially viable due to low oxidation potentials and/or poor stability in their oxidized (radical cation) state.[14] Increasing the oxidation potentials of redox shuttles whilst maintaining radical cation stability is particularly challenging. The radical cation form of a redox shuttle is subject to dimerization reactions and/or nucleophilic attack due to its radical nature and electron deficiency.[15] Introducing electron-withdrawing groups to increase oxidation potentials often further destabilizes the radical cation form by

making it even more electron deficient. For redox shuttles to be used with high voltage cathode materials,[13,16–18] it is necessary to develop stable redox shuttles with higher oxidation potentials.

N-Alkylphenothiazine derivatives were reported as redox shuttles by the Dahn group; this class of compounds exhibits overcharge protection for a relatively large number of overcharge cycles, yet are limited in application due to their low oxidation potentials (*ca.* 3.5 V *vs.* Li[+/0]).[19,20] We are interested in incorporating electron-withdrawing substituents onto the aromatic backbone of N-alkylated phenothiazines to increase their oxidation potentials for use with high voltage cathodes.

In designing derivatives of N-alkylated phenothiazines, we sought to place these substituents at more reactive positions of the phenothiazine core to improve stability in the radical cation form. Aromatic amines such as triphenylamines and phenothiazines are subject to dimerization and oligomerization reactions in the radical cation state, which has been shown to occur most readily at the positions *para* to the nitrogen atoms.[21–26] Conveniently, these positions are the most reactive in electrophilic aromatic substitution reactions, making them easy to modify with a variety of substituents. Therefore, for this study, we synthesized 3,7-disubstituted derivatives of EPT in which substituents are incorporated at the positions *para* to the nitrogen atoms (Fig. 1). We introduced electron-withdrawing substituents (–Cl, –Br, –CF₃, and –CN) for consideration with higher oxidation potential derivatives for high voltage cathodes. In one case we incorporated an electron-donating substituent (–CH₃) to block the *para* positions without decreasing electron density in the aromatic ring.

The synthesis of 3,7-disubstituted derivatives of EPT was accomplished in two or three steps from phenothiazine (Scheme S1, ESI†). Briefly, phenothiazine was alkylated with bromoethane yielding EPT, which was then chlorinated with N-chlorosuccinimide to synthesize DClEPT or brominated with N-bromosuccinimide to synthesize DBrEPT. Next DBrEPT was treated with n-butyllithium followed by iodomethane to produce DMeEPT, potassium trifluoroacetate to produce BCF3EPT, or copper cyanide to produce DCNEPT. All products were characterized by standard spectroscopic techniques. Single crystal X-ray structures were obtained for EPT, DMeEPT, and

Department of Chemistry, University of Kentucky, Lexington, KY 40506-0055, USA.
E-mail: susan.odom@uky.edu; Fax: +1-859-323-1069; Tel: +1-404-805-1799

† Electronic supplementary information (ESI) available: Experimental procedures, ^{1}H and ^{13}C NMR spectra, mass spectra, elemental analysis, cyclic voltammograms, X-ray crystallographic data, and coin cell cycling results. CCDC 963734–963736. For ESI and crystallographic data in CIF or other electronic format see DOI: 10.1039/c3cc47503d
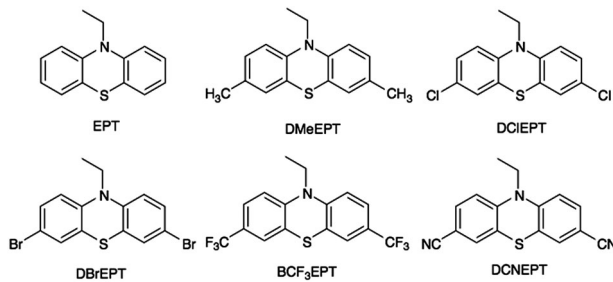
Fig. 1 N-Ethylphenothiazine (EPT) and derivatives 3,7-dichloro-N-ethyl-phenothiazine (DClEPT), 3,7-dibromo-N-ethylphenothiazine (DBrEPT), 3,7-dimethyl-N-ethylphenothiazine (DMeEPT), 3,7-bis(trifluoromethyl)-N-ethyl-phenothiazine (BCF3EPT), and 3,7-dicyano-N-ethylphenothiazine (DCNEPT).

DCNEPT (Fig. S1–S3, Table S2, ESI†). As expected, the benzene rings deviate from planarity at the N and S positions, with dihedral (Φ) angles ranging from 134.6° to 156.6°, a feature often observed in phenothiazine derivatives.[27–31]

DFT calculations were performed for EPT and the disubstituted derivatives using the B3LYP/6-31G** basis set[32,33] to predict molecular geometries and adiabatic ionization potentials, and thus predict the trend in oxidation potentials. Relative oxidation potentials were also predicted using Hammett constants of the *para* substituents, using two times the value of the Hammett constants because the EPT derivatives contain two substituents, consistent with a previous study of ferrocene derivatives.[34] Cyclic voltammetry (CV) experiments were used to determine oxidation potentials in dichloromethane (DCM) containing 0.1 M nBu$_4$NPF$_6$ and in ethylene carbonate–ethyl methyl carbonate (EC–EMC) (3 : 7 wt%) containing 1.2 M LiPF$_6$, a common battery electrolyte. The voltammograms in both electrolytes are shown in Fig. 2. Expanded versions containing the internal reference Cp*$_2$Fe are shown in the ESI† (Fig. S5).

Cyclic voltammograms show that all compounds exhibit reversible oxidations in both electrolytes. We know from our recent study that reversibility in CV does not necessarily correlate with overcharge performance; voltammograms were used only to determine oxidation potentials.[35] As expected, the oxidation potentials of the disubstituted EPTs increase with electron-withdrawing substituents (–Cl, –Br, –CF$_3$, –CN) and decrease with the electron-donating
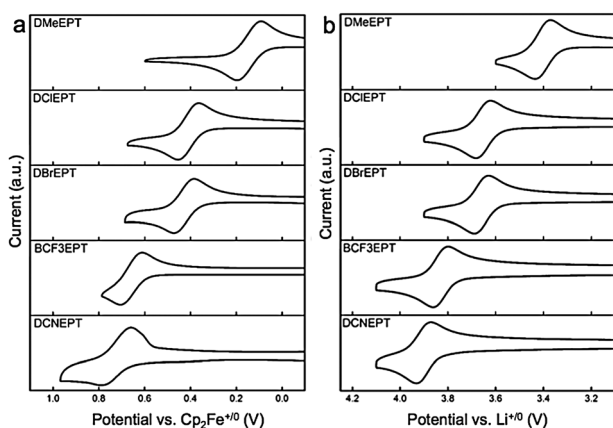
Table 1 Hammett constants, calculated adiabatic IPs, half-wave oxidation potentials ($E_{1/2}^{+/0}$) vs. Cp$_2$Fe$^{+/0}$ in 0.1 M nBu$_4$NPF$_6$ in DCM and vs. Li$^{+/0}$ in 1.2 M LiPF$_6$ in EC/EMC (3/7), and number of overcharge cycles achieved in synthetic graphite/LiFePO$_4$ coin cell batteries

Redox shuttle	Substituent Hammett const (σ_p)	Calculated adiabatic IP (eV)	$E_{1/2}^{+/0}$ vs. Cp$_2$Fe$^{+/0}$ (V)	$E_{1/2}^{+/0}$ vs. Li$^{+/0}$ (V)	Number overcharge cycles
DMeEPT	–CH$_3$; –0.17	6.14	0.13	3.40	36, 48, 83
EPT	–H; 0	6.37	0.27	3.51	20, 27, 65
DClEPT	–Cl; 0.23	6.65	0.41	3.64	19, 22, 37
DBrEPT	–Br; 0.23	6.60	0.43	3.66	2, 4, 5
BCF3EPT	–CF$_3$; 0.54	6.91	0.61	3.83	17, 75, 95
DCNEPT	–CN; 0.66	7.20	0.73	3.90	0, 0, 1

The asterisk next to some values in the number of overcharge cycles indicates that the battery was still cycling at the time of manuscript submission and the number provided indicates the current cycle number.
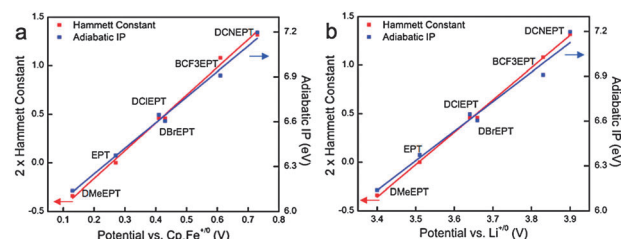

Fig. 3 Plots of the oxidation potentials of redox shuttle candidates vs. Cp$_2$Fe$^{+/0}$ (a) and vs. Li$^{+/0}$ (b) with Hammett constants (2 × σ_p) and calculated adiabatic IPs with their respective linear fits for Hammett constants (red) and adiabatic IPs (blue).

substituent (–CH$_3$). Numerical values for the oxidation potentials in both electrolytes, calculated adiabatic IPs, and Hammett constants (σ_p) are reported in Table 1. In both electrolytes there is a linear correlation between oxidation potentials and Hammett constants as well as with calculated adiabatic IPs (Fig. 3).

To test overcharge performance, we assembled and cycled synthetic graphite/LiFePO$_4$ coin cells containing EPT and the disubstituted derivatives as electrolyte additives at 0.08 M in 1.2 M LiPF$_6$ in EC–EMC (3 : 7). Although cycling data for EPT has been reported by Dahn and coworkers,[19] we tested the overcharge performance of EPT to serve as a benchmark for our laboratory. Overcharge performance varies with redox shuttle concentration, electrolyte composition, and electrode materials, so for consistency, comparisons in redox shuttle performance should be performed in the same battery environment.[19,20] The number of overcharge protection cycles observed for each additive in multiple coin cells is reported in Table 1. We report all cycle numbers (not an average or maximum number of cycles) to show the variation in results that occurs in overcharge testing results.[36]

The overcharge protection exhibited by the EPT derivatives showed variable results. DMeEPT shows voltage stabilization for a relatively large number of overcharge cycles (Fig. 4a) but – given its lower oxidation potential – oxidizes before the battery is fully charged. DClEPT (Fig. 4b) and DBrEPT (Fig. S6, ESI†) both exhibited overcharge protection although with fewer overcharge cycles than EPT or DMeEPT. We hypothesize that DClEPT and DBrEPT decompose more rapidly due to their more polarizable carbon–halogen bonds, which could easily cleave to form radical species. BCF3EPT survived for more overcharge cycles than either halogenated derivative (Fig. 4c), despite having a higher oxidation potential. This result is
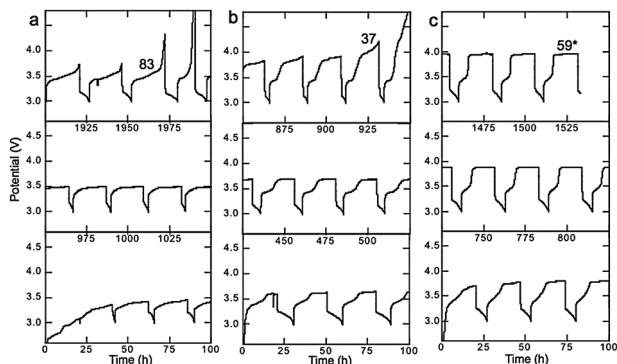

Fig. 2 Cyclic voltammograms of disubstituted EPT derivatives in 0.1 M nBu$_4$NPF$_6$ in dichloromethane vs. Cp$_2$Fe$^{+/0}$ at 0 V (a) and in 1.2 M LiPF$_6$ in EC–EMC (3 : 7) vs. Li$^{+/0}$ at 0 V (b). Both contain Cp$_2$*Fe as the internal reference (not shown) and were recorded at 100 mV s^{-1}.

Fig. 4 Overcharge cycling at 100% overcharge (100% more charge than cell charge capacity) of synthetic graphite/LiFePO₄ coin cell batteries containing 1.2 M LiPF₆ in EC–EMC (3 : 7) and 0.08 M DMeEPT (a), 0.08 M DClEPT (b), and 0.08 M BCF3EPT (c). *The BCF3EPT battery is still cycling.

consistent with the polarizability being an important factor in radical cation stability, since the C–CF₃ bond is less polarizable than the C–Cl and C–Br bonds. At overcharge cycle number 95, one of the BCF3EPT coin cells is still cycling as of submission of this manuscript.[37] Lastly DCNEPT exhibited little to no overcharge protection, which may be due to the oxidation potential of the derivative becoming too high, perhaps resulting in a radical cation that is too reactive to survive in the battery electrolyte. When an aromatic ring becomes significantly electron deficient, it may be subject to nucleophilic attack as a method of decomposition.[15] EPT radical cations have been shown to be stabilized by interactions with neutral equivalents in a donor–acceptor π dimers at concentrations of 0.5 mM. It is also possible that the radical cations of electron poor derivatives like DCNEPT are not stabilized by their neutral counterparts, leading to lower stability of these radical cations at higher concentrations in battery electrolyte (0.08–0.10 M) compared to electron rich versions. Rigorous investigation of mechanisms for decomposition and their effect on variation in overcharge performance is the subject on ongoing research to be published at a later date.

In summary, 3,7-disubstituted derivatives of EPT were synthesized as redox shuttle candidates, modified using electron-donating and electron-withdrawing substituents to vary their oxidation potentials, particularly in an effort to synthesize redox shuttles for use with high voltage cathodes. Hammett constants and DFT calculations of adiabatic IPs were both reliable techniques for predicting the oxidation potentials of the EPT derivatives, as the values from each result showed a linear correlation with measured oxidation potentials. Consistent with previous results, we observed that reversibility of oxidations measured using CV does not correlate to trends in overcharge performance; voltammograms show reversible oxidations for all EPT derivatives despite the significant variation in overcharge performance. Lastly, all but one disubstituted EPT derivative protects batteries from overcharge, with BCF3EPT being the most promising candidate for high voltage cathodes.

Notes and references

1 Y.-K. Sun, S.-T. Myung, B.-C. Park, J. Parakash, I. Belharouak and K. Amine, *Nature*, 2009, **8**, 320.
2 L. Zhang, Z. Zhang, P. C. Redfern, L. A. Curtiss and K. Amine, *Energy Environ. Sci.*, 2012, **5**, 8204.
3 S.-I. Tobishima and J. I. Yamaki, *J. Power Sources*, 1999, **81–82**, 882.
4 P. Biensan, B. Simon, J. P. Peres, A. de Guibert, M. Broussely, J. M. Bodet and F. Perton, *J. Power Sources*, 1999, **81–82**, 906.
5 Z. Chen, Y. Qion and K. Amine, *Electrochim. Acta*, 2009, **54**, 3603.
6 P. G. Balakrishnan, R. Ramesh and T. P. Kumar, *J. Power Sources*, 2006, **155**, 401.
7 S. S. Zhang, *J. Power Sources*, 2006, **162**, 1379.
8 J. W. Wen, Y. Yu and C. H. Chen, *Mater. Express*, 2012, **2**, 197.
9 C. Buhrmester, J. Chen, L. Moshurchak, J. Jiang, R. L. Wang and J. R. Dahn, *J. Electrochem. Soc.*, 2005, **152**, A2390.
10 J. Chen, C. Buhrmester and J. R. Dahn, *Electrochem. Solid-State Lett.*, 2005, **8**, A59.
11 M. Taggougui, B. Carre, P. Willmann and D. Lemordant, *J. Power Sources*, 2007, **174**, 643.
12 L. M. Moshurchak, W. M. Lamanna, M. Bulinski, R. L. Wang, R. R. Garsuch, J. W. Jiang, D. Magnuson, M. Triemert and J. R. Dahn, *J. Electrochem. Soc.*, 2009, **156**, A209.
13 L. Zhang, Z. Zhang, H. Wu and K. Amine, *Energy Environ. Sci.*, 2011, **4**, 2858.
14 Z. Zhang, L. Zhang, J. A. Schlueter, P. C. Redfern, L. A. Curtiss and K. Amine, *J. Power Sources*, 2010, **195**, 4957.
15 M. Schmittell and A. Burghart, *Angew. Chem., Int. Ed. Engl.*, 1997, **36**, 2550.
16 J. M. Tarascon and M. Armand, *Nature*, 2001, **414**, 359.
17 S. Patoux, L. Daniel, C. Bourbon, H. Lignier, C. Pagano, F. L. Cras, S. Jouanneau and S. Martinet, *J. Power Sources*, 2009, **189**, 344.
18 M. Hu, X. L. Pang and Z. Zhou, *J. Power Sources*, 2013, **237**, 229.
19 C. Buhrmester, L. Moshurchak, R. L. Wang and J. R. Dahn, *J. Electrochem. Soc.*, 2006, **153**, A288.
20 C. Buhrmester, L. Moshurchak, R. L. Wang and J. R. Dahn, *Electrochim. Acta*, 2007, **52**, 3379.
21 H. D. Zhao, C. Tanjutco and S. Thayumanavan, *Tetrahedron Lett.*, 2001, **42**, 4421.
22 R. J. Bushby, C. A. Kilner, N. Taylor and M. E. Vale, *Tetrahedron*, 2007, **63**, 11458.
23 L. M. Moshurchak, C. Buhrmester and J. R. Dahn, *J. Electrochem. Soc.*, 2008, **155**, A129.
24 O. Yurchenko, D. Freytag, L. zur Borg, R. Zentel, J. Heinze and S. Ludwigs, *J. Phys. Chem. B*, 2012, **116**, 30.
25 A. N. Pankratov, I. M. Uchaeva and A. N. Stepanov, *Can. J. Chem.*, 1993, **71**, 411.
26 S. Zh. Ozkan, G. N. Bondarenko, A. V. Orlov and G. P. Karpacheva, *Polym. Sci., Ser. B*, 2009, **51**, 855.
27 J. McDowell, *Acta Crystallogr., Sect. B*, 1976, **32**, 5.
28 S. S. C. Chu and D. Helm, *Acta Crystallogr., Sect. B*, 1975, **31**, 1179.
29 C. S. Kramer and T. J. J. Muller, *Eur. J. Org. Chem.*, 2003, 3534.
30 H. Wang, W. Xu and B. Zhang, *J. Chem. Crystallogr.*, 2012, **42**, 846.
31 M. Malinska, J. Novacki, A. Kapturkiewicz and K. Wozniak, *RSC Adv.*, 2012, **2**, 4318.
32 C. Lee, W. Yang and R. G. Parr, *Phys. Rev. B*, 1988, **47**, 785.
33 A. D. Becke, *J. Chem. Phys.*, 1993, **98**, 5648.
34 M. N. Ates, C. J. Allen, S. Mukerjee and K. M. Abraham, *J. Electrochem. Soc.*, 2012, **159**, A1057.
35 S. A. Odom, S. Ergun, P. P. Poudel and S. R. Parkin, *Energy Environ. Sci.*, DOI: 10.1039/C3CC47503D.
36 The variation in results may be due to inconsistencies in electrode thicknesses or to batteries being fabricated on different days, which could result in using different ages of battery electrolyte of different ages or slightly different oxygen and water content in the glove box. When possible, we fabricate batteries on the same day as one another to minimize potential changes in battery environment.
37 We will report the number of overcharge cycles for the currently cycling BCF3EPT batteries in a future publication.